bioresources.com

Short-Term Creep Behavior of CFRP-Reinforced Wood Composites Subjected to Cyclic Loading at Different Climate Conditions

Xiaojun Yang,[a,*] Meng Gong,[b] and Ying Hei Chui [b]

Carbon fiber reinforced plastic (CFRP) was used to adhesively reinforce Chinese fir (*Cunninghamia lanceolata*) wood specimens. This study examined the flexural static and creep performances of CFPR-reinforced wood composites that had been subjected to changes in moisture and stress levels. The major findings were as follows: 1) the cyclic creep was slightly lower for those specimens subjected to the cyclic stress condition than for those subjected to a constant stress level due to the deflection recovery under cyclic loading; 2) the environmental conditions of high temperature and high humidity assisted in accelerating the creep by increasing the moisture content of the composite and reducing the compressive strength of wood, causing the composite specimen to fail *via* damage in the wood layer from compressive crushing; 3) the stress level governed the creep of the CFRP-reinforced wood composite; and 4) the Burger model was able to accurately simulate the short-term creep performance of the CFPR-reinforced wood composite. It was suggested the maximum bending stress level should be limited to 40% for the CFRP-reinforced wood composites fabricated in this study.

*Contact information: a: College of Material Science and Engineering, Nanjing Forestry University, Nanjing, 210037, China; b: Wood Science & Technology Center, University of New Brunswick, Fredericton, E3C 2G6, Canada; *Corresponding author: yxj5460@163.com*

INTRODUCTION

Chinese fir (*Cunninghamia lanceolata*) is one of the most commonly used wood species in China due to its abundant availability, rapid growth, and ease of processing. However, Chinese fir is not typically well utilized in the wood industry because its relatively low wood density yields soft wood having a loose texture. These disadvantages limit its applications, especially in the field of timber engineering, which requires high stiffness and strength. To overcome these shortcomings, Chinese fir wood must be modified *via* reinforcement technologies. The use of carbon fibers to improve the mechanical properties of low-density wood has shown great potential. One effective technique involves adhesively bonding carbon fiber-reinforced plastic (CFRP) onto a wood surface in order to manufacture a CFRP-reinforced wood composite with improved mechanical performance. Twenty years ago, CFRP had just been used successfully to reinforce a historic wood bridge near Sins in Switzerland (Meier *et al*. 1992). Pre-stressed timber beams with glass fiber-reinforced plastic (GFRP) and CFRP have also been used at the Horrem Community Centre in Germany and in a tea house in Japan (Nanni 1993). The use of CFRP to reinforce existing timber floors was studied by Schober in 2006. The above success stories have attracted more and more researchers and manufacturers.

In a study by Tingley (1996), glued laminated timber was reinforced with a 13-layer structure made of Douglas fir (*Pseudotsuga menziesii*) by bonding CFRP panels of 0.86 mm thickness onto the outermost tension layer using an epoxy adhesive. The dimensions of each beam specimen were 130 mm in width, 305 mm in depth, and 4 m in length. In the same study, strain tests were conducted on wood and CFRP laminates based on an application of the 4-point load bending test to a beam specimen with a span-to-depth ratio of 12:1. It was found that localized strength variations, such as the slope of the grain, knots, and finger joints in the tension laminate adjacent to the CFRP of a specimen, were the major causes of failure. In a study by Triantafillou (1997), CFRP sheets of thickness 0.167 mm were bonded, using an epoxy adhesive, to the critical shear stressed areas of the side edge of a section of Norway spruce (*Picea abies*) to fabricate composite beam specimens. The beam's dimensions were 65 mm in width, 100 mm in depth, and 600 mm in length, with the exception of the shear spans, where the width was intentionally reduced to 25 mm to ensure that shear failure would be the governing mode. Four configurations were used: one CFRP sheet at 0° (*i.e.*, the direction parallel to the grain), one sheet at 90° (*i.e.*, the direction perpendicular to the grain), two sheets at 0°, and two sheets at $0^o/90^o$. Shear tests were conducted on the beams shortly after they had been subjected to 4-point bending over a span of 500 mm. It was found that the shear strength of the CFRP reinforcement with two sheets at 0° was the highest and that the shear strength of the reinforcement with one sheet at 90° was the lowest. The two mentioned beams were found to have shear strengths 42% and 4.8% higher, respectively, than unreinforced beams. The efficiency of CFRP reinforcement depended on the CFRP configuration and area fraction. In a study by Li (2009), CFRP sheets were bonded onto the tension surface of wood beam specimens composed of Chinese fir (*Cunninghamia lanceolata*) or Chinese hemlock (*Tsuga chinensis*) using an epoxy adhesive. The dimensions of the beam specimens were 1.1 m in length, 65 mm in width, and 65 mm in depth. A 4-point bending test was conducted, and it was found that the modulus of rupture (MOR) values for the Chinese fir retrofitted with 1, 2, and 3 layers of CFRP composite sheets were 39%, 44%, and 61% greater, respectively, in comparison to those without the CFRP sheet. Moreover, the MOR values were 44%, 55%, and 58% greater for the Chinese hemlock retrofitted with 1, 2, and 3 layers of CFRP composite sheets than for those without the CFRP sheets. In a study by Jankowski *et al.* (2010), CFRP (with a thickness of 1.2 mm)-reinforced Scots pine (*Pinus sylvestris*) wood beams were constructed that were 120 mm in width, 220 mm in thickness, and 4 m in length. 4-point bending tests were conducted at a span-to-depth ratio of 17.3:1, and the strain distribution images tests were captured using a photoelastic coating technique. It was found that the MOR and modulus of elasticity (MOE) of the reinforcement significantly depended on the quality of the wood-CFRP strip bond. In a study by Gezer and Aydemir (2010), CFRP was adhesively wrapped around Silver fir (*Abies alba*) wood beams with dimensions of 20 mm in width, 20 mm in depth, and 300 mm in length. Compression and bending tests were conducted, and it was found that the compressive strength and MOR values of reinforced specimens were 66% and 65% higher, respectively, than those of un-reinforced specimens.

It is well known that wood used in construction exhibits notable creep behavior under sustained loads, and such creep has a significant effect on the safety and service-ability of wood structures over their lifetime. Researchers have been studying time-dependent creep behavior for decades, and some methods of these investigations have included subjecting small or large specimens to constant or cyclic climate conditions as

well as subjecting specimens to constant or cyclic stress levels (Bodig and Jayne 1982; Hoyle *et al*. 1985; Yang 1990; Toratti and Svensson 2000; Svensson and Toratti 2002; Fortino *et al*. 2009). Many of the creep characteristics and behaviors of most wood species have been thoroughly documented, giving rise to the classical creep models and advanced creep models. For example, Hanhijärvi and Mackenzie-Helnwein (2003) established a viscoelastic-mechanosorptive-plastic model with hygroexpansion for wood subjected to high-temperature drying process, which was applicable over a wide range of temperatures as well as moisture content (20 to 100 ^{o}C; nearly 0% moisture content to fiber saturation). However, studies on the creep behavior of CFRP-reinforced wood have been limited. Plevris and Triantafillou (1995) examined the creep behavior of lowland fir (*Abies grandis*) beams of dimensions 1664 mm in length, 45 mm in width, and 86 mm in depth. The beams had been reinforced with CFRP that was bonded to the tension faces using epoxy and then had been subjected to the three-point bending test. The team developed, based on the Burger model and the mechano-sorptive concept, an analytical method for calculating the deformation of a beam under constant environmental conditions. It was found that environmental temperature and humidity had a great influence on the creep of the specimens. Shen and Gupta (1997) evaluated the creep behavior of Douglas fir (*Pseudotsuga menziesii*) beams with dimensions of 38.1 mm in width, 88.9 mm in depth, and 2.44 m in length in a natural environment and found that the four-element model could be expanded to take into account the impacts of beam stiffness and air temperature, which fit the experimental data well. Jia and Davalos (2006) explored the use of artificial neural networks (ANN) to study the fatigue of interfaces between glass fiber-reinforced polymer (GFRP) composites and red maple (*Acer rubrum* L.) wood, which were bonded using a phenolic adhesive. Fatigue crack growth rate tests were conducted on contoured double cantilever beam (CDCB) specimens under load control. It was found that the fatigue test could characterize the long-term performance of bonded interfaces, and the ANN model was proposed as a predictor of critical fatigue responses, such as crack growth rate, that would facilitate the development of design guidelines for hybrid material bonded interfaces.

This study investigated the short-term cyclic creep behavior of CFRP-reinforced wood composites that were subjected to three stress levels, two loading sequences, and two climate conditions. Chinese fir was chosen as the test material. For comparison purposes, static and creep tests were conducted as well.

EXPERIMENTAL

Materials and Specimens

The wood species used in the study was Chinese fir (*Cunninghamia lanceolata*), and the specimens selected had an air-dry density of 0.357 g/cm^{3} and an average moisture content of 15%. Only quarter-sawn lumber segments, having dimensions of 2 m in length, 200 mm in width, and 25 mm in depth, were used. The CFRP was a unidirectional fabric polyacrylonitrile, each sheet of which had a nominal thickness of 0.111 mm, a surface density of 206 g/m^{2}, a tensile modulus of elasticity of 2.4×10^{5} MPa, a tensile strength of 3450 MPa, and an ultimate tensile strain of 1%. The adhesive used was a two-component epoxy which, at 23 ^{o}C, had a mixed initial viscosity of 5000m Pa·s in a ratio of 2:1. The basic properties of the cured epoxy were a tensile strength of 50 MPa, a modulus of elasticity of 2.0 GPa, and an extensibility of 2.2%.

The CFRP-reinforced wood composite was fabricated as follows. First, a CFRP sheet was laid onto polyvinyl chloride film (PVC). Second, the two-component epoxy resin was mixed and spread over the surface of the CFRP sheet using a roller, then allowed to penetrate the adhesive for 3 min. Third, the adhesive-penetrated CFRP sheet was laid onto the wide face of the lumber such that the glued surface faced the wood. Caution was used to avoid the formation of bubbles between the bonding layers. Fourth, the opposing face of each CFRP sheet was also coated with epoxy. Finally, the composite was pressed in a cold press until the epoxy had cured. A piece of PVC was inserted between the composite and the platen of the press. The manufacturing parameters used were as follows: resin content of 250 g/m^2, pressing pressure of 0.10 MPa, and pressing time of 48 h. The dimensions of each specimen were 300 mm in length, 20 mm in width, and 20 mm in depth. A total of 21 composite specimens were made, which were grouped into 7 sets. For comparison purpose, 30 solid wood specimens of the same dimensions were prepared. All the specimens were stored in a conditioning chamber at a temperature of 20 ^{o}C and a relative humidity of 65% prior to testing.

Static and Creep Testing

The static three-point bending tests were conducted, using a universal testing machine (Model: UTM5105), on both solid wood and CFRP-wood composite specimens under the 'normal' condition, which consisted of a temperature of 20 ^{o}C and relative humidity of 65% in accordance with the Chinese National Standard (GB/T 1936.1-2009). The purpose of the tests was to obtain the maximum bending load and therefore determine the stress level for the creep tests. The testing span was 240 mm and the loading speed was 2 mm/min. The crosshead movement, load, and elapsed time were all recorded during testing.

The stress levels used in the creep tests corresponded to 20%, 40%, and 50% of the average bending stress levels at failure. Two cyclic loading schedules were applied in the creep tests: 20% to 40% and 20% to 40% to 50%, as seen in Fig. 1. The loading time at each stress level was 1 h, and the total loading time was 24 h. In addition, two specified climate conditions were used during the creep tests to examine the effects of the moisture content of wood on the creep behavior: (1) a 'dry' condition with a temperature of 24 °C and a relative humidity of 45% and (2) a 'wet' condition with a temperature of 60 ^{o}C and a relative humidity of 90%. The equivalent moisture contents of wood during the 'dry' and 'wet' conditions were 9.9% and 18.0%, respectively. The equilibrium moisture content for the 'dry' condition would be reached in 10 min and for the 'wet' condition in 15 min from the 'normal' condition (T= 20, RH= 65 %).
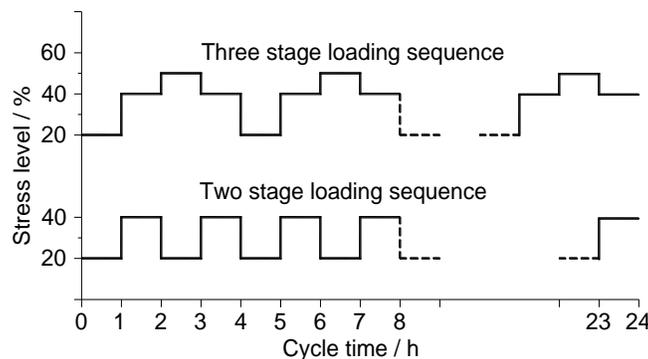

**Fig. 1.** Loading schedules used in creep tests

Table 1 gives the design of the experiment used in this study. In total, there were two sets for the static tests and eight sets for the creep tests. The creep tests were carried out using a universal testing machine (GDS-100/UTM4304), which was equipped with a conditioning chamber with a temperature range from 0 to 100 ^{o}C and relative humidity range of 15% to 98%. The specified load was applied in the load control mode during loading and unloading segments at a rate of 2 mm/min, and was kept constant for each hour during the creep. The data were logged at a frequency of 3.0 Hz at the stress level transition stage and at a frequency of 0.5 Hz.

Table 1. Design of Experiment for Static and Creep Tests

Loading type	Set Code	Material	Stress level / %	Environmental condition	Replicates
Static	SW	Wood	——	Normal	30
Static	SC	Composite	——	Normal	30
Creep	W-40	Wood	40	Dry	3
Creep	CG-40	Composite	40	Dry	3
Creep	CS-40	Composite	40	Wet	3
Creep	CS-50	Composite	50	Wet	3
Creep	CG-20-40	Composite	20-40	Dry	3
Creep	CS-20-40	Composite	20-40	Wet	3
Creep	CG-20-40-50	Composite	20-40-50	Dry	3
Creep	CS-20-40-50	Composite	20-40-50	Wet	3

Creep Model Analysis

The creep of wood and wood composites, which consists of instantaneous elastic deformation, delayed elastic deformation, and viscous deformation, is widely modeled using the Burger model (Bodig and Jayne 1982; Hoyle *et al.* 1985; Yang 1990), *i.e.*, the four-component model consisting of springs and dashpots that can be seen in Fig. 2.
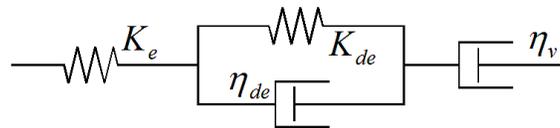
Fig. 2. Burger model

The Burger model is expressed in Eq. 1,

$$\varepsilon = \sigma\left[\frac{1}{K_e} + \frac{1}{K_{de}}\left(1 - e^{-\frac{K_{de}}{\eta_{de}}t}\right) + \frac{t}{\eta_v}\right] \tag{1}$$

where σ is the stress applied (Pa), ε is the creep strain, K_e and K_{de} are the instantaneous and delayed elastic moduli (N/mm^2), respectively, η_v is the viscosity coefficient for the permanent strain (N·min /mm^2), η_{de} is the viscosity coefficient (N·min /mm^2), and t is the loading time (min). To facilitate calculation, equation (1) can be simplified into Eq. 2,

$$Y(t) = A_1 + A_2\left[1 - \exp(-A_3 t)\right] + A_4 t \tag{2}$$

where $Y(t)$ denotes deflection (mm) at time t (min); t is the creep time (min); A_1 through A_4 are the undetermined coefficients, with A_1 (mm) and A_4 (mm/min) reflecting the elastic deformation and viscous deformation, respectively, while A_2 (mm) and A_3 (min^{-1}) reflect the viscoelastic deformation.

In this study, the viscoelastic behavior of CFRP-wood composite specimens was simulated using the Burger model. Due to the small depth of specimen (*e.g.* 20 mm) and wood rings perpendicular to the reinforced surface, the effects of hygro-thermal expansion and the effects of mechanosorption for the cases with climate conditions were not taken into account in Eq. 2. Therefore, the average deflection of each set of specimens was used to determine the model parameters (Eq. 2) using the nonlinear fitting method *via* Origin8.0 software (OriginLab Corporation 2008).

RESULTS AND DISCUSSION

Static Test

Table 2. Summary of the Load at Failure in Bending

Material	Mean / N	Coefficient of variation (COV) / %
Wood	674	10.16
CFRP-Wood Composite	1057	6.52

Table 2 gives the means and COVs of the loads at failure of wood and CFRP-wood composite specimens. The average load at failure of the CFRP-wood composite specimens was 1.57 times larger than that of the wood specimens. However, the COV of the composite was about 40% lower than that of wood, suggesting that the composite had uniform structure and properties. Figure 3 illustrates the load-deflection curves of both the composite and the wood specimens that were tested in bending.
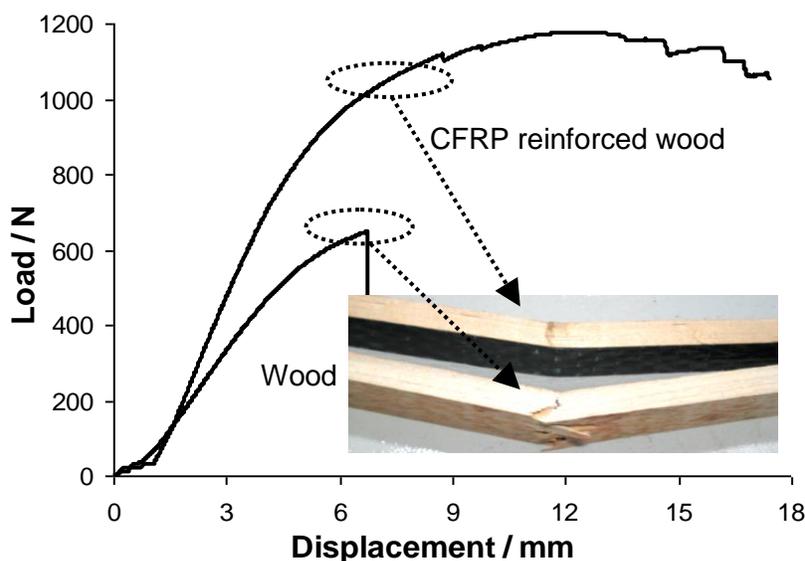

Fig. 3. Typical load-deflection curves of wood and composite specimens in bending

bioresources.com

In the case of the composite, the load increased linearly with the increase in deflection and decreased gradually after reaching the peak load, suggesting that the composite exhibited ductile behavior. As for the solid quarter-sawn wood specimen, however, a sudden drop in load was observed after the peak load, which indicated some brittle fracture. The difference in fracture behavior between the composite and the wood was attributed to the use of CFRP, which improved the mechanical properties of the tension side of the composite specimen. This was further verified by the occurrence of compression failure in the composite specimen (Fig. 3).

Creep Test Analysis

Each creep curve in Figs. 4, 6, and 7 represents the average response of three specimens in a group. In addition, the fitting curve of each group plotted in these figures is constructed on the basis of the deflection data points by using the nonlinear fitting method *via* Origin8.0 software. Figure 4 shows the four average creep curves representing the four testing groups. Creep consists of three phases: primary, secondary, and tertiary creep (Bodig and Jayne 1982). From Fig. 4, it can be seen that two phases occurred in groups CG40, W-40, and CS-40, and three phases occurred in group CS-50. During primary creep, the creep increased very quickly over the course of 55 min for CG-40 and W-40, over 120 min for CS-40, and over 110 min for CS-50. Obviously, these four curves can be classified into three groups based on stress level and moisture content. In the secondary phase, the creep increased slowly over time in groups CG-40 and W-40 and quickly in group CS-40. It appeared that group CS-50 was an exception. After passing through a short and non-obvious primary phase, the creep of CS-50 entered a subsequent phase and increased very quickly, after which it transitioned from the secondary to tertiary phase, ultimately causing the failure of the specimen at 965 min. This pattern of behavior could be attributed to the higher stress level (*i.e.*, 50%) and the higher moisture content (*i.e.*, 18%) applied to group CS-50 in comparison to the other three groups. And the presence of moisture-induced stresses generated by moisture gradients in wood was another important reason (Fortino *et al.* 2009).
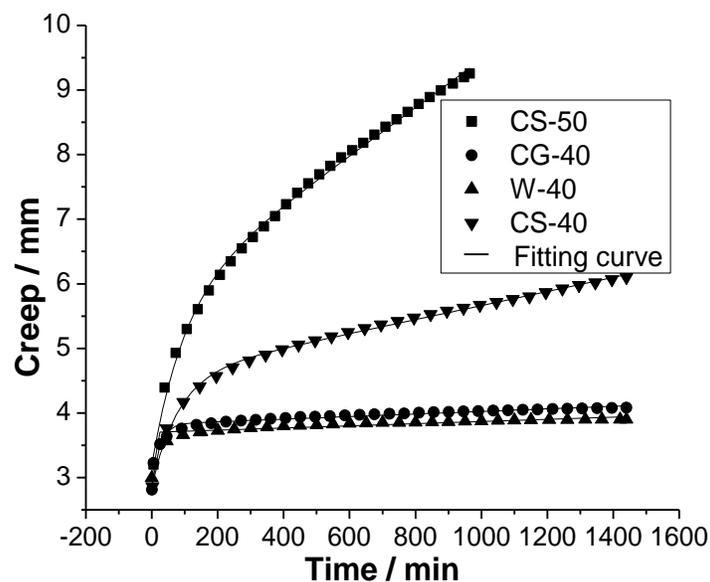

Fig. 4. Creep curves and fitting curves of wood and composite specimens at a constant stress level

It can be seen in Fig. 4 that at the same stress level and moisture content, the creep of group CG-40 (the composite specimens) was slightly greater than that of group W-40 (the solid wood specimens). This may have occurred because the contribution of the compressive deformation in wood in both types of specimens governed the creep at the level of stress applied (*i.e.*, 40%), which was about 35% lower than the proportional limit. At the same stress level but under different environmental conditions, the creep curves of groups CG-40 and CS-40 were comparable during the primary phase (*i.e.*, instantaneous elastic deformation) but differed notably during the secondary creep phrase. The creep at 24 h in the wet condition (*i.e.*, group CS-40) was 1.56 times larger than that in the dry condition (*i.e.*, group CG-40). This difference in creep was attributable to the difference in moisture content between these two groups. After a CS-40 specimen was placed in the testing chamber under conditions of 60 ^{o}C and 90% relative humidity for 24 h, the moisture content of the specimen increased, eventually reaching about 18% despite there being an inhomogeneous distribution of moisture in specimens, *i.e.*, 8.1% higher than that in the dry condition. Under the coupling action of both temperature and moisture, most of the mechanical properties of wood decreased (Forest Products Laboratory 2010). Because of the decrease in the bending strength of wood and the presence of moisture-induced stresses generated by moisture gradients in wood, the constant load applied actually increased significantly the stress level that added on the composite. In addition, the reduced stiffness of the wood composite specimens resulted in increased creep, which was in agreement with the findings of Plevris (1995), who showed that the creep behavior of CFRP-reinforced wood was primarily dominated by the creep of the wood, especially at high environmental temperature and humidity conditions. Under the same wet conditions, the creep of group CS-50 (loaded at a 50% stress level) was much higher than that of group CS-40 (loaded at a 40% stress level). Tertiary creep appeared in group CS-50, *i.e.*, failure happened after 965 min on average. It was observed during compressive testing that the wood in the composite specimen became crushed, as shown in Fig. 5, suggesting that at a stress level of 50% in the wet condition, the compressive stress exceeded the compressive strength of the wood in the composite specimen.
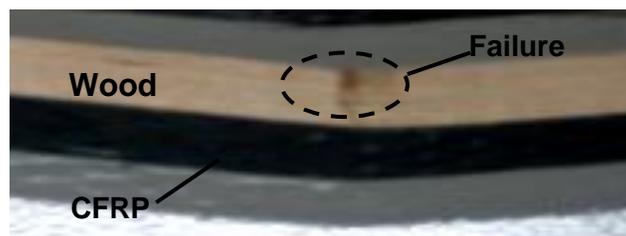
Fig. 5. Creep failure of a CS-50 specimen tested in wet condition

Figure 6 shows the creep curves of the specimens tested at various loading sequences and under various environmental conditions. Under the dry condition, the creep curves were similar across all three groups (*i.e.*, CG-20-40, CG-40, and W-40). It should be noted that the creep curve of group CG-20-40 was formed by connection of the peak deflections at each load cycle. It appeared that the creep of group CG-20-40 was slightly lower than that of CG-40. This might have been due to the recovery of a CG-20-40 specimen during the cyclic loading at the stress level of 20%.
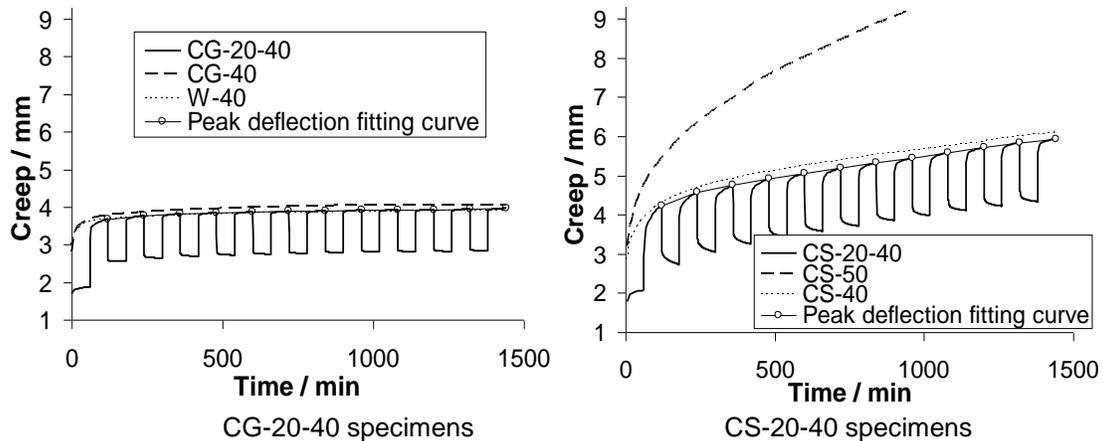
Fig. 6. Creep and fitting curves of specimens CG-20-40 (left) and CS-20-40 (right)

Under the wet condition, a similar trend as that under the dry condition could be found between the two groups (*i.e.*, CS-20-40 and CS-40) for the curves. It appeared that the creep of CS-20-40 was also slightly lower, due to the deflection recovery under cyclic loading, than that of CS-40. The group CS-50 had relatively higher creep than did the other groups because a higher stress level of 50% had been applied.

It can be seen in Fig. 6 that under the same cyclic loading sequence, the creep curves of CG-20-40 and CS-20-40 behaved in a similar way. At the initial stage of loading, at the stress level of 20%, the creep increased gradually with time. When the stress level was switched to 40%, the creep increased over a short period of time (20 min) and then continued to grow gradually over time while the stress level remained at 40%. When the stress level was switched to 20% in the following cycle, the creep decreased sharply, signalling an instantaneous elastic recovery, and then decreased with time, which was reflective of a delay in elastic recovery after having experienced the high stress level (*i.e.*, 40%). However, for the same stress level, the valley creep value in one cycle was slightly larger than that in the previous cycle. It is also evident that the peak creep value for each cycle gradually increased with each additional increase in cyclic loading. It can be seen in Fig. 6 that the creep growth rate under the wet condition was apparently larger than that during the dry condition due to the coupling influence of moisture and temperature, which could generate mechanosorptive creep (Svensson and Toratti 2002; Fortino *et al*. 2009; Hanhijärvi and Mackenzie-Helnwein 2003). It was also observed that all the specimens subjected to a two-phase cyclic loading sequence survived over 24 h.

Figure 7 shows the creep curves of the specimens tested at various loading sequences and environmental conditions. Under the dry condition, the creep curves were similar across all three groups (*i.e.*, CG-20-40-50, CG-40, and W-40). It appeared that the creep of CG-20-40-50 was slightly higher than that of CG-40. This may have been due to the unrecovered deflection during creep of a specimen subjected to cyclic loading at the stress level of 50%. Under the wet condition, there were significant differences in creep among the three groups (*i.e.*, CS-20-40-50, CS-40, and CS-50).

It appeared that the creep of CS-20-40-50 was greater than that of CS-40 but lower than that of CS-50. This could be attributed to the stress level applied. Under the wet condition, the 50% stress level was already capable of causing damage to a specimen, generating compressive damage, as previously mentioned. The failure of specimens was observed at the center of the wood compressive area.
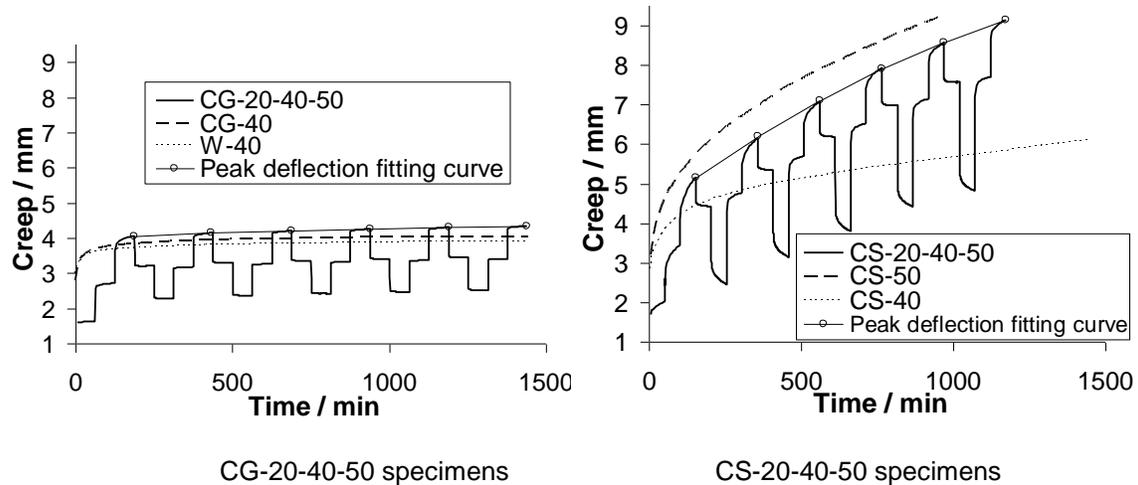
CG-20-40-50 specimens   CS-20-40-50 specimens

Fig. 7. Creep and fitting curves of specimens CG-20-40-50 (left) and CS-20-40-50 (right)

Under the same cyclic loading sequence, the creep of those specimens under the dry condition in each cycle grew slowly; however, under the wet condition, the creep increased quickly, resulting in failure after about 1173 min. The composite specimens at the higher stress level of 50% demonstrated lower resistance to temperature and humidity than those at 40%.

From Figs. 4, 6, and 7 and the above discussion, the stress level, moisture, and temperature all played a critical role in the creep of those specimens subjected to the cyclic loading. After 1389 min, the creep of CG-20-40-50 at a stress level of 50% was 9.6% larger than that of CG-20-40 at 40%. CS-20-40-50 failed at 1173 min, indicating that tertiary creep had appeared.

In a few words, the loading time, temperature, humidity, peak stress level, and cycling sequence were all found to be important factors affecting the creep of CFRP-reinforced wood composites fabricated in this study. High climate temperature and humidity assisted in accelerating the creep by increasing the moisture content of the composite, reducing the compressive strength of wood and adding additional mechano-sorptive creep and hygroexpansion, causing failure of the composite specimen during compressive crushing. The stress level governed the creep of the composite.

Fitted Data Analysis

Table 3. Model Parameters Determined Using the Nonlinear Fitting Method

Set code	Environment condition	A_1	A_2	A_3	A_4	R^2
W-40	Dry	2.99463	0.74298	0.02736	0.00013	0.98995
CG-40	Dry	2.88887	0.93541	0.04239	0.0002	0.98052
CS-40	Wet	2.86879	1.7062	0.01229	0.00109	0.99753
CS-50	Wet	3.18004	2.56929	0.01028	0.00372	0.99767
CG-20-40	Dry	3.44666	0.37224	0.00732	0.0001	0.99918
CS-20-40	Wet	3.60695	0.8255	0.00783	0.00106	0.99950
CG-20-40-50	Dry	3.95672	0.17994	0.00278	0.00015	0.99974
CS-20-40-50	Wet	4.20822	3.21026	0.00146	0.00198	0.99995

The Burger creep model can be used to describe the average creep of a group of specimens at a given testing condition. The non-linear fitting method was employed to determine the model parameters, *i.e.*, A_1, A_2, A_3, and A_4, in Equation (2). Table 3 lists these model parameters, from which it can be found that the coefficients of determination (R^2) are all greater than 0.98, indicating an excellent correlation between the test data and fitting curve of each group of specimens. A_1, A_2, A_3, and A_4 represent instantaneous deformation within the elastic region, delay elastic deformation, viscoelastic deformation, and viscous creep deformation, respectively, of the material, variables that are associated with the stress level applied, loading sequence, and environmental conditions (*i.e.*, temperature and relatively humidity). From Table 3, it can be found that the A_1 of group CS-40 (*i.e.*, the 40% stress level) was about 10% lower than that of group CS-50 (*i.e.*, the 50% stress level). As for the specimens at two-stage or three-stage stress levels, A_1 was determined by the initial peak stress level. A_1 was also influenced by the moisture content of the specimens. The A_1 of group CS-20-40 (*i.e.*, the wet condition) was slightly larger than that of group CG-20-40 (*i.e.*, the dry condition). It was also found that 1) the A_2 of group CS-50 (*i.e.*, the 50% stress level) was 50% larger than that of group CS-40 (*i.e.*, the 40% stress level); and 2) the A_2 of group CS-40 (*i.e.*, the wet condition) was 80% larger than that of group CS-40 (*i.e.*, the dry condition). The A_3 of the dry condition was larger than that of the wet condition. The A_3 of the low stress level was larger than that of the high stress level. A_2 and A_3 indicated that the stress level was greater when the ability to recover the original deformation of a specimen exposed to the wet environment decreased, *i.e.*, when the degree of damage of this specimen increased. When A_4 increased, the unrecovered deformation for a specimen increased as well.

In summary, all of the model parameters in Eq. 2 were associated with peak stress level, loading sequence, and climate condition. When the stress level increased, A_1, A_2, and A_4 increased significantly, and A_3 decreased slightly. When the moisture content of a specimen was increased, A_1, A_2, and A_4 increased significantly, and A_3 decreased slightly. To some degree, the model parameters could reflect the effect of these influencing factors. The short-term creep characteristics of CFRP-reinforced wood composites could be accurately described using the Burger model. But the mode couldn't reflect mechanosorptive creep with hygroexpansion. It is recommended that the new mode of viscoelastic-mechanosorptive with hygroexpansion should be established based on the Burger mode for future studies.

CONCLUSIONS

1. The short-term cyclic creep of CFRP-reinforced wood composite specimens that had been subjected to changes in moisture and stress level consisted of two or three creep phases: primary, secondary, and tertiary. The coupling action of both temperature and moisture added additional mechanosorptive creep and hygroexpansion, making a non-obvious primary phase and shortening the secondary and tertiary phase separately.

2. The loading time, temperature, humidity, peak stress level, and cycling sequence were important factors affecting the creep of CFRP-reinforced wood composite specimens. The stress level governed the creep of the composite. High climate temperature and humidity accelerated the creep mainly by reducing the compressive strength of wood and generating mechanosorptive creep, causing failure in the wood

bioresources.com

layer of the CFRP-reinforced wood composite specimens during the compressive crushing.

3. When the stress cycle was set to 1 h and peak stress levels were kept the same, the creep of the CFRP-reinforced wood composite specimens subjected to the cycle stress condition was slightly lower than the creep of those subjected to the constant stress level, a difference attributed to the deflection recovery under cyclic loading.

4. Because all of the model fitting coefficients of correlation (R^2) were greater than 0.98, it was determined that the short-term creep characteristics of CFRP-reinforced wood composites in dry or wet environments could be accurately described using the Burger model. All of the model parameters were governed by the peak stress level, loading sequence, and environmental conditions.

5. Although Chinese fir wood bonded with CFRP was able to reach a high flexural strength, the creep characteristic could not be significantly improved due to the crush damage that occurred in the wood on the compression side of the composite specimens. It is recommended that the maximum bending stress level should be limited to 40% for the CFRP-reinforced wood composite fabricated in this study.

ACKNOWLEDGMENTS

REFERENCES CITED

Bodig, J., and Jayne, B. A. (1982).*Mechanics of Wood and Wood Composites*, U.S. National Agricultural Library, Van Nostrand Reinhold, New York.

China National Standard. (2009). GB/T 1936.1-2009. "Wood bending strength test method," *China National Standardization Management Committee*, China.

Forest Products Laboratory. (2010). *Wood Handbook: Wood as an Engineering Material*, U.S. Dept. Agri. For. Prod. Lab., Madison, WI.

Fortino, S., Mirianon, F., and Toratti, T. (2009). "A 3D moisture-stress FEM analysis for time dependent problems in timber structures," *Mech. Time-Depend. Mater.* 13(4), 333-356.

Gezer, H., and Aydemir, B. (2010). "The effect of the wrapped carbon fiber reinforced polymer material on fir and pine woods," *Materials and Design* 31(7), 3564-3567.

Hanhijärvi, A., and Mackenzie-Helnwein, P. (2003). "Computational analysis of quality reduction during drying of lumber due to irrecoverable deformation. I: Orthotropic viscoelastic-mechanosorptive-plastic material model for the transverse plane of wood," *Journal of Engineering Mechanics* 129(9), 996-1005.

Hoyle, R. J., Griffith, M. C., and Itani, R. Y. (1985). "Primary creep in Douglas fir beams of commercial size and quality," *Wood Fiber Science* 17(3), 300-313.

Jankowski, L. J., Jasienko, J., and Nowak, T. P. (2010). "Experimental assessment of CFRP reinforced wooden beams by 4-point bending tests and photoelastic coating technique," *Materials and Structures* 43(2), 141-150.

Jia, J. H., and Davalos, J. F. (2006). "An artificial neural network for the fatigue study of bonded FRP-wood interfaces," *Composite Structures* 74(1), 106-114.

Li, Y. F., Xie, Y. M. and Tsai, M. J. (2009). "Enhancement of the flexural performance of retrofitted wood beams using CFRP composite sheets," *Construction and Building Materials* 23(1), 411-422.

Meier, U., Deuring, M., Meier, H., and Schwegler, G. (1992). "Strengthening of structure with CFRP laminates: Research and applications in Switzerland," *1st Int. Conf. on Advanced Compos. Mat. in Bridges and Struct.*, Montreal, Canada, pp.243-251.

Nanni, A. E. (1993). *Fiber-reinforced Plastic Reinforcement for Concrete Structures: Properties and Applications*, Elsevier, Amsterdam.

OriginLab, OriginPro 8 SR4. (2010). OriginLab Corporation, Northampton, MA.

Plevris, N., and Triantafillou, T. C. (1995). "Creep behavior of FRP-reinforced wood members," *Journal of Structural Engineering* 121(2), 174-186.

Schober, K. U., and Rautenstrauch, K. (2006). "Post-strengthening of timber structures with CFRPs," *Materials and Structures* 40(1), 27-35.

Shen, Y. H., and Gupta, R. (1997). "Evaluation of creep behavior of structural lumber in a natural environment," *Forest Products Journal* 47(1), 89-96.

Svensson, S., and Toratti, T. (2002). "Mechanical response of wood perpendicular to grain when subjected to changes of humidity," *Wood Science and Technology* 36, 145-156.

Tingley, D. A. (1996). "The stress-strain relationships in wood and fiber-reinforced plastic laminate of reinforced glued-laminated wood beams," *PhD dissertation*, Oregon State University, Corvallis.

Toratti, T., and Svensson, S. (2000). "Mechano-sorptive experiments perpendicular to grain under tensile and compressive loads," *Wood Science and Technology* 34, 317-326.

Triantafillou, T. C. (1997). "Shear reinforcement of wood using FRP materials," *Journal of Materials in Civil Engineering* 9(2), 65-69.

Yang, T. Q. (1990). *Viscoelastic Mechanics*, Huazhong University of Science and Technology (HUST) Press, Wuhan, China.